International Journal of Control and Automation
Vol.8, No.8 (2015), pp.349-362
http://dx.doi.org/10.14257/ijca.2015.8.8.33

Parametric Design and Efficiency Analysis of the Output-Pin-Wheel Cycloid Transmission

Junhua Bao and Weidong He

Department of Mechanical Engineering, Dalian Jiaotong University
bao_junhua@aliyun.com, hwd@aliyun.com

Abstract

By analyzing the shortcomings of various types of cycloid drives, a kind of drive was innovated, which was named as output-pin-wheel cycloid drive. Using the pin-wheel as output part is the biggest different of this kind of drive compared with traditional cycloid reducer. The construction of reducer was redesigned for its specific transmission structure, and corresponding structures and dimensions of parts were designed by analyzing their working principles and design methods. In order to validate the working performance of this drive and check assembly relations of parts, three-dimensional solid models and its assembly model were built. It was done that the force analysis of input shaft and output shaft. The strength calculations and finite element analysis of transmission parts were calculated also. We analyzed the method of efficiency calculation and derived the calculation equations.

Keywords: *Output-pin-wheel cycloid drive; Virtual prototyping; Parametric design; Transmission efficiency*

1. Introduction

It is known that the cycloid planetary drive is provided with a series of essential advantages, such as multi-teeth mesh and hardened tooth surface, small volume and light weight, wide range of transmission ratio and steady transmission, high efficiency and low noise, etc [1, 2]. So it has a wide applications and take large proportion of reducer products, such as using in universal reducer and RV reducer, etc [3-5]. Using its advantages such as multi-teeth meshing and hardened teeth surface, the carrying capacity of cycloid planetary drive should be great, but it has not been utilized fully in traditional drive. The main reasons include two aspects. First, the size and life of bearings are restricted by the dimensions of the cycloidal gears and output mechanism, because the rotating bearings of planetary gears are placed inside the output mechanism. Second, the output mechanism is designed as a kind of cantilever structure, hence the stiffness of output shaft is reduced and the rotational accuracy of output shaft can't be guaranteed. In the other way the shortcomings of involute planetary drives are reserved in the double or three rings involute planetary reducer that has been widely used in China. The contact ratio is too small for involute planetary reducer, not only limits its loading capacity, but also affects the transmission stability. The transmission angle is too large, which not only reduces the life of bearings, which but also reduces its efficiency. All above weakness become the obstacle, so the carrying capacity of all involute drives is restricted [6, 7]. At the same time, ring-plate-type reducers can't be designed as axial symmetry structure for the structural requirements, so large dynamic loading, vibration and noise are generated during the working process. Although the carrying capacity of ring-plate type reducers has been increased linearly, the weight of product is also increased [1, 2].

ISSN: 2005-4297 IJCA
Copyright ⓒ 2015 SERSC

By integrating above advantages and disadvantages we proposed a kind of cycloid planetary drive that was named as output-pin-wheel cycloid drive [8]. The drive retains advantages of traditional cycloid planetary types, and improves the working condition of bearings by adopting more reasonable structure. The loading capacity of output-pin-wheel cycloid drive is improved because the stiffness and strength of output shaft is increased by structural innovation, and we use more pieces of cycloidal gears than traditional type for force balance. In this paper we finished the parametric design, 3D solid modeling, force analysis and FEA, efficiency analysis for this kind of drive to explain its advantages and characters.

2. Parametric Design

Parametric design offers a new paradigm in the field of Computer-Aided Design, which associates engineering knowledge with geometry and topology in the product model by means of constraints [9-11]. The goal of the parametric design is to improve the performance of a product or the efficiency of a design process. A lot of researches about parametric design had been done about principles and algorithms, kinds of equipments and constructions use parametric design as an efficient tool [12-14]. For the case of this thesis we will select a few parameters that influent the structure of this drive and strength of main parts, and then we will discuss the structural design and parametric design of the output-pin-wheel cycloid drive.

2.1. Structure Design

The kinematics diagrams of mechanisms are shown in Figure 1. It is the traditional cycloid drive that is shown in Figure 1.a, the other is the type of output-pin-wheel cycloid drive.

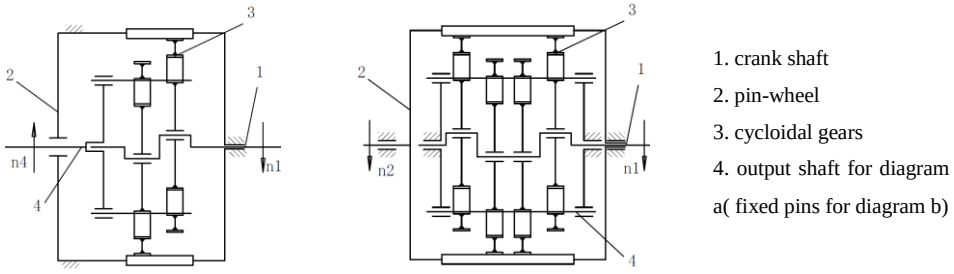

a. traditional style b. output-pin-wheel style

Figure 1. Kinematics Diagrams of Cycloid Drives

The main differences of these two kinds of drives are two aspects. First, output-pin-wheel cycloid drive uses four pieces of cycloidal gears as transmission parts, which act as the third component in Figure 1, but traditional style uses two pieces of gears usually, so the new type can transfer more power, and the symmetrical structure of new type can ensure the balance of force and bending moment of input-shaft. All the gears support on the input shaft that is the first component in Figure 1. Second, all fixed-pins pass through the holes on the cycloidal gears and are fixed on the box of the output-pin-wheel reducer, but in the structures of traditional style similar parts as fixed-pins make up the output component. The rotation of the every cycloidal gear around its axis is restricted by the fixed-pins, but the revolution of gears around input shaft is free, at the same time gears mesh with pin-wheel and transfer the motion and power by driving the output shaft (pin-wheel and output shaft make up the output component). According to the calculating method of transmission ratio of planetary gear trains we obtain the ratio $i_{12} = \frac{\omega_1}{\omega_2} = \frac{z_p}{z_p - z_c}$ for

 Copyright ⓒ 2015 SERSC

output-pin-wheel cycloid drive [8, 15-17], where z_c is the teeth number of cycloidal gear and z_p is the teeth number of pin-wheel.

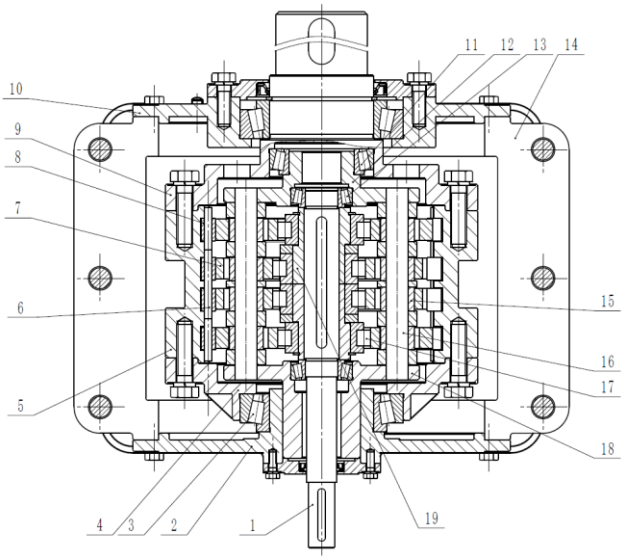

Figure 2. Structural Diagram of Output -pin-wheel Cycloid Reducer

For the purpose of fitting the structural requirements of four cycloidal gears, improving the rigidity and strength of output shaft and fixed-pins, we redesigned the structure of reducer, which is shown in Figure 2. The main characteristics of reducer include: the input shaft insert into the reducer through the center hole of part 18 and is supported on a pair of bearings 13. Two eccentric sleeves are assembled on the input shaft by keys. The sleeves make up a kind of mirrored structure each other (if the eccentricity is very short, the manufacture of eccentric sleeves would be difficult. Hence, crankshaft would be a more appropriate structure than eccentric sleeve and input shaft). Two sets of gear and rotary arm bearing are assembled on an eccentric sleeve that is a kind of double eccentric symmetrical structure about axis of input shaft. The cycloidal gears are assembled on the rotary arm bearings, and the bearings are assembled on eccentric sleeves. The cycloidal gear makes the planetary motion driven by the input shaft, at the same time contacts with fixed-pin bushings through fixed-pin-holes on the gear. Four fixed-pin bushings are assembled on the corresponding location of each fixed-pin. All fixed-pins are assembled in the holes of both sides of fixed-pin support flanges. Four gears mesh with pin-bushings, and drive the pin-wheel and output shaft indirectly. The pin-bushing is assembled on the pin. The pins are assembled on the pin-wheel, so the pin-wheel can rotate and export the motion and torque. The stable supported structures of input shaft, output shaft and fixed-pins are obtained. Hence, the rigid and loading capacity of reducer would be improved compared with traditional type.

2.2. Parametric Design

The software system of parametric design is compiled by referencing design methods of classical cycloid planetary drive and considering structural characteristics of output-pin-wheel cycloid reducer. The basic parameters of prototype are listed in Table 1. Teeth number of pin-wheel z_p is equal to the transmission ratio of reduce. The parameters and dimensions of cycloidal gear are calculated based on the basic parameters. The calculation system provides basic functions of strength checking and dimensions calculation.

Copyright ⓒ 2015 SERSC

Table 1. Basic Parameters of Prototype of Output-pin-wheel Cycloid Drive

Teeth number of cycloidal gear z_c	28
Teeth number of pin-wheel z_p	29
Eccentric distance a （mm）	2
Diameter of assembly circle of pins d_p （mm）	174
Diameter of pin-bushing d_{rp} （mm）	11
Width of cycloidal gear b （mm）	16
Power P （KW）	7.5
Rotation speed of input shaft n （r/min）	1750
Transmission ratio i	29

In theory, the number of meshing teeth between pin-wheel and gear is half teeth of cycloidal gear. It is not the more teeth are contacted, the better working condition is. In fact, the profile of cycloidal gear will be modified during design and manufacture, so the number of contact teeth is less than $z_c/2$. It is necessary to know how much modification of profile is reasonable for the purpose of getting ideal working condition and high transmission efficiency. One interface of force calculation and strength checking program is listed in Figure 3. It is shown that there are six teeth of gear are contacted with pins of pin-wheel at the same time. The maximum force is appeared on the fourth tooth, and the force is 1,083 N. The radial force act on pitch point of cycloidal gear is about F_r=515 N, the circumferential force is about F_t=5,361 N, the operating pressure angle is 5.487°.

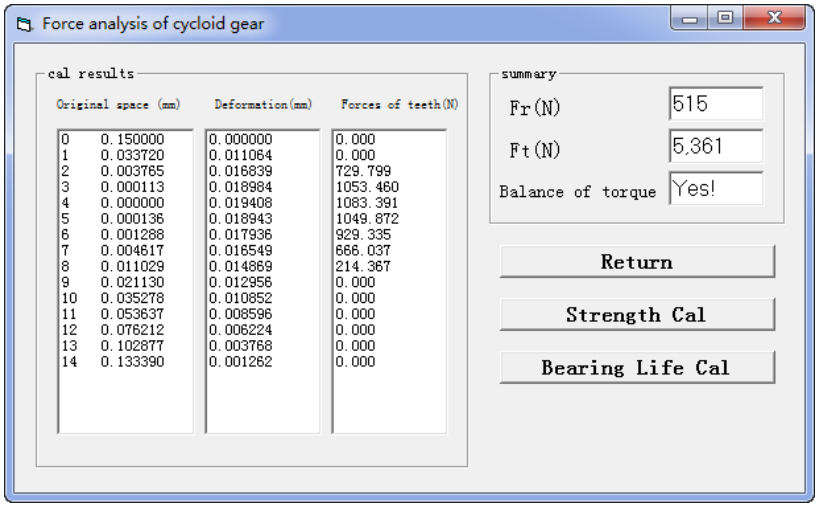

Figure 3. Force Analysis Result of Cycloidal Gear and an Interface of Software

2.3. 3D Computer Aided Design

Using 3D CAD software system, we built 3D solid models of cycloid reducer. The functions of cycloid profile coordinate are defined by Eq.1. Using the

Copyright ⓒ 2015 SERSC

parameters listed in Table 1 and Eq.1, we build the cycloid curve through command Curve by Functions in Pro/E software.

$$\begin{cases} x_c = [r_p + \Delta r_p - (r_{rp} + \Delta r_{rp})(1 + K_1^2 - 2K_1 \cos\varphi)^{-1/2}] \\ \cos[(1 - z_p / z_c)\varphi] - \dfrac{a}{r_p + \Delta r_p}[r_p + \Delta r_p - z_p(r_{rp} + \Delta r_{rp}) \\ (1 + K_1^2 - 2K_1 \cos\varphi)^{-1/2}]\cos(z_p \cos\varphi / z_c) \\ y_c = [r_p + \Delta r_p - (r_{rp} + \Delta r_{rp})(1 + K_1^2 - 2K_1 \cos\varphi)^{-1/2}] \\ \sin[(1 - z_p / z_c)\varphi] + \dfrac{a}{r_p + \Delta r_p}[r_p + \Delta r_p - z_p(r_{rp} + \Delta r_{rp}) \\ (1 + K_1^2 - 2K_1 \cos\varphi)^{-1/2}]\sin(z_p \cos\varphi / z_c) \end{cases} \quad (1)$$

Where, Δr_p is the amount of displacement profile modification, and Δr_{rp} is the amount of pin profile modification, and $K_1 = \dfrac{a}{r_{rp} + \Delta r_{rp}}$.

The model of cycloid gear is shown in Figure 4.a. Figure 4.b shows the final model of gear. The central hole is assembly placement of rotary arm bearing, and the small holes are assembly holes of fixed-pins.

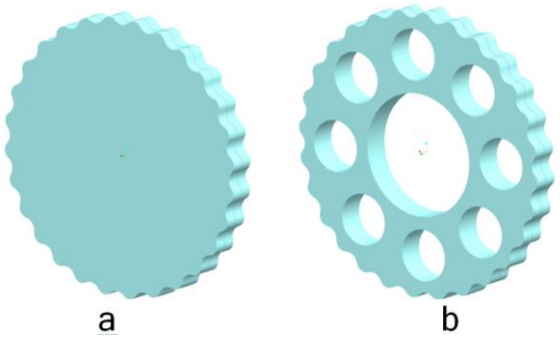

Figure 4. 3D Solid Model of Cycloidal

That manufacture high performance prototype and finish the laboratory test is the most effective means for proving the superiority of product. But the cost is high and design cycle is long. Hence, the virtual prototype technology is a kind of new development of product-oriented CAX technology and manufacture-oriented DFX technology [18-20]. All these technologies will be integrated in the design and manufacture of complex system. That the virtual prototype substitute physical prototype used in innovation design and performance test and assessment is to shorten the development cycle, reduce product costs and improve product design quality and the adapting ability about the market and customers.

By analyzing working principles and characteristics of drive, the kinematics and dynamics simulation of drive has been done, and virtual prototype of drive is obtained [9]. As an improving type of existing virtual prototype, the structure of reducer is built in 3D CAD software system, at the same time the interference checking of parts are done, and the positional relationship of parts is shown in Figure 5. Figure 5.a is the exploded diagram of drive, and the assembly drawing of 3D solid models is shown in Figure 5.b.

Copyright ⓒ 2015 SERSC

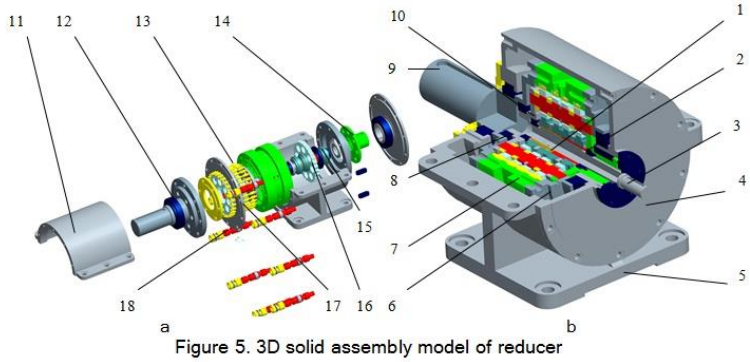

Figure 5. 3D solid assembly model of reducer

1. eccentric sleeves (two sleeves are symmetrically arranged)
2. bearings of input shaft
3. input shaft
4. bearing cover of input shaft
5. box
6. pin-wheel support flange (input side)
7. pin-wheel
8. fixed-pins support bearing
9. output shaft
10. fixed-pin support flange of output shaft side
11. cover box
12. bearings of output shaft
13. pins and pin-bushings
14. fixed-pin support flange of input shaft side
15. rotary arm bearing
16. cycloidal gears (four pieces)
17. bearing cover of output shaft
18. fixed-pins and fixed-pin bushings

Figure 5. 3D Solid Assembly Model of Reducer

The 18 sets of main parts are marked in Figure 5, and we can find their assembly relations clearly. First, the eccentric sleeves, rotary arm bearings, cycloidal gears are assembled on the input shaft sequentially along axial direction, and we can assemble the support bearings and constraint parts on their design locations. And then the fixed-pins that are assembled with fixed-pin bushings are assembled in the holes of cycloidal gears, and the two support flange 10 and 14 are assembled two sides of fixed-pins by holes and pins, at the same time the bearing 2 on the input side is assembled in the bearing hole of part 14, and the other bearing is assembled in the hole of part 10. We call the assemblies that are assembled already as assembly A. Secondly, zp sets of pins that are assembled with pin bushings beforehand are assembled in the holes of pin-wheel, and the assembly A is assembled into the pin-wheel as shown in Figure 5.b, and on the two sides of pin-wheel we will join the flange 6 and output shaft 9 by bolts that are distributed in the circumferential direction, and then assemble two bearing 12 on the output shaft and part 6. We call the assemblies as assembly B. Finally, assembly B is support on the box that is made by part 4, part 5, part 11 and part 17 by support bearings 12.

3. Force Analysis and Calculations of Strength

The output-pin-wheel cycloid reducer is a kind of developing type of pin cycloidal planetary drive, the structural characteristics and advantages of pin cycloidal planetary drive determine the excellent capability that achieve the static and dynamics balance in working condition. Based on the design requirements, the calculations of strength of pins and fixed-pins, working life of bearings and strength of cycloidal gears are done after accurate force analysis and finite element analysis.

3.1. Force Analysis and Strength Calculations of Cycloidal Gears

At the upper section about the parameters design, the force relationship between the pins and cycloidal gear is showed in Figure 3. It is shown that the force of the 4th tooth of cycloidal gear is the biggest. After calculating correspondingly, the contact stress, bending stress and rotate deformation can be known from the Table 2.

Copyright ⓒ 2015 SERSC

Table 2. Strength Calculations of Cycloidal Gear

Contact stress of tooth of gear $\sigma_{H\max}$ (MPa)	887.5
Bending stress of pin $\sigma_{F\max}$ (MPa)	124.4
Rotate deformation of pin $\theta_{\max}$ (rad)	0.0015
Force of support bearing of planetary gear F_H (N)	5865.8
Angle between F_H and crank α_{Fx} (°)	66.059
Life of planetary gear supported Bearing L_{h} (h)	13652

3.2. Force Analysis of Crank Shaft

The crank shaft as apart of input shaft is supported by two bearings, which is shown in Figure 2. The reaction loads between gears with rotary arm bearings are act on the crank shaft through two eccentric sleeves, as shown in Figure 6. The force direction between sleeves with input shaft is changed along with the rotation of input shaft cyclically, so the reaction force of support points A and B are changed also.

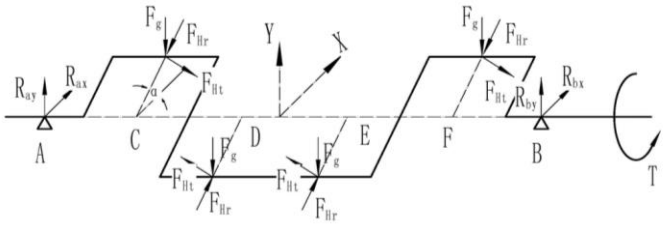

Figure 6. Force Diagram of Input Shaft

Where the angle between eccentric direction of shaft and Axis X is defined as angle α, which is changed between 0-2π rad. Here we defined anticlockwise as positive. Where the reaction forces FH are increased by 5% after considering the unbalanced load as a kind of simplified calculation. Hence the force analysis result of input shaft is defined by Eq.2.

$$\begin{cases} \sum F_x = 0 \quad R_{ax} + R_{bx} = 0 \\ \sum F_y = 0 \quad R_{ay} + R_{by} - 4 \cdot F_g = 0 \\ \sum M_x(A) = 0 \quad (F_{Ht} \cdot \sin\alpha - F_{Hr} \cdot \cos\alpha) \cdot (L_{CD} - L_{EF}) - R_{bx} \cdot L_{AB} = 0 \\ \sum M_y(A) = 0 \quad \begin{array}{l} (F_{Ht} \cdot \cos\alpha + F_{Hr} \cdot \sin\alpha) \cdot (L_{EF} - L_{CD}) + \\ F_g(4L_{AC} + 3L_{CD} + 2L_{DE} + L_{EF}) - R_{by} \cdot L_{AB} = 0 \end{array} \end{cases} \tag{2}$$

Where R_{i} is reaction force, F_{g} is weight of gear, F_{H} is force between gear with bearings, which can be decomposed to $F_{\mathrm{Ht}}=F_{\mathrm{H}}\cdot\sin\alpha_{\mathrm{Fx}}$ and $F_{\mathrm{Hr}}=F_{\mathrm{H}}\cdot\cos\alpha_{\mathrm{Fx}}$.

The structural characteristics of drive which ensure the assembly placement of cycloidal gears on input shaft symmetrically. Hence, the length $L_{\mathrm{EF}}=L_{\mathrm{CD}}$. If we ignore the weight of shaft and inertial loads, the forces and moments would be balanced. Reaction forces that are acted on point A and B can be calculated by $R_{ax} = R_{bx} = 0$, $R_{ay} = R_{by} = 2F_{\mathrm{g}}$. The gravitational force F_{g} is much smaller than contact forces between bearings with gears, hence, the reaction forces exerting on bearings are small and the working life is enough. Although the reaction forces are

small, bending moments is not equal to zero everywhere on input shaft, and the maximum bending moment is acted on point E that is shown in Figure 6, and the calculation result of moment is listed in Table 2. And then, structural design of shaft is done also.

The crank shaft is simplified as a simply supported beam in classical force analysis, so the stress concentration can't be analyzed accurately. FEM analysis will be used in this kind of drive for stress and structural calculations [21-24]. The input shaft, eccentric sleeves and key are import into ANSYS as a finite element model, which is shown in Figure 7.a. Conditions of constraint and force include: First, we restrict the freedoms of point A that include radial and axial directions. And then we restrict the freedom of radial direction of point B. Second, circumferential force F_{Ht} and radial force F_{Hr} are set on loading nodes, which are corresponding points C, D, E and F in Figure 6. Finally, we set the input torque on the nodes of model and output the stress and displacement distribution of input shaft as shown in Figure 7.b and Figure 7.c.

The calculating conditions and analysis results of crankshaft are listed in Table 3. The calculating bending moment of input shaft is 177,647 $N \cdot mm$ by Eq.2. The bending stress is about 92 MPa by calculating. Result of FEA is 259 MPa, the maximum stress distribute in the point A and B that is shown in Figure. 7b. There are two main stress concentration places on the shaft.

Table 3. Calculating Conditions and Analysis Results of Crank Shaft

Circumferential force F_{Ht} (N)	5,361
Radial force F_{Hr} (N)	2,380
Input torque T ($N \cdot mm$)	42,888
Maximum bending moment of input shaft M_{Emax}($N \cdot mm$)	175,800
Calculating moment M_{vmax} ($N \cdot mm$)	177,647
Bending stress of theory calculation (MPa)	92
Maximum stress of FEA (MPa)	259
Maximum displacement of FEA (mm)	0.236

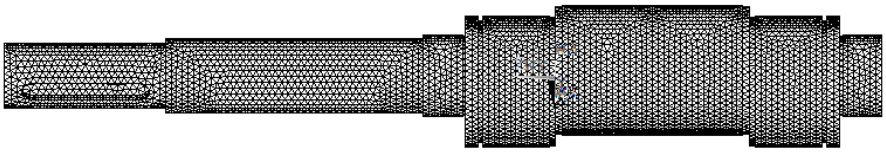

a. finite element model of crank shaft

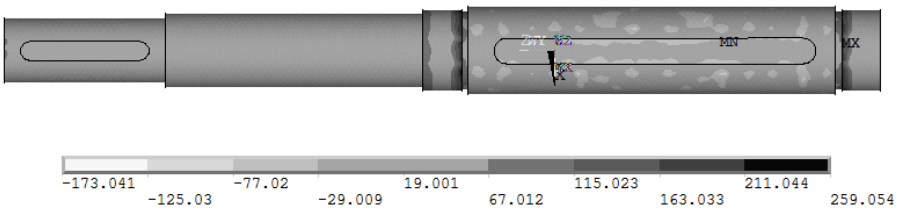

b. stress result of input shaft

Copyright ⓒ 2015 SERSC

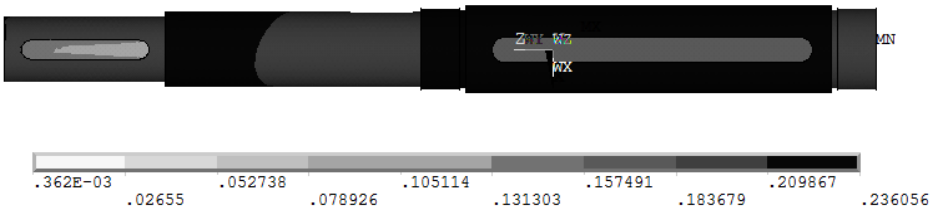

c. displacement result of input shaft

Figure 7. Finite Element Analysis of Crank Shaft

3.3. Force Analysis of Output Shaft

The output component is made up by output shaft, pin-wheel, supported flange, pins and pin-bushings. Pin-wheel is jointed with output shaft and supported flange by bolts, and the component is supported on two bearings. As the major part in structure of output component, the pin-wheel meshes with four cycloidal gears simultaneously by pins on it. The diagram of force analysis is shown in Figure 8, the contact forces acting on the pin-wheel is decomposed to F_r and F_t. Those forces act on the pitch circle of pin-wheel, and action points of forces are changed along with rotation of output shaft cyclically. The angle between the direction of Fr and the Axis X is defined as angle β.

The force analysis of output shaft can be expressed by

$$\begin{cases} \sum F_x = 0 \quad R_{gx} + R_{mx} = 0 \\ \sum F_y = 0 \quad R_{gy} + R_{my} - F_g{}' = 0 \\ \sum M_x(G) = 0 \quad (F_t \cdot \sin\beta - F_r \cdot \cos\beta) \cdot (L_{HI} - L_{JK}) - R_{mx} \cdot L_{GM} = 0 \\ \sum M_y(G) = 0 \quad (F_t \cdot \cos\beta + F_r \cdot \sin\beta) \cdot (L_{JK} - L_{HI}) + F_g{}' \cdot L_{GN} - R_{my} \cdot L_{GM} = 0 \end{cases} \tag{3}$$

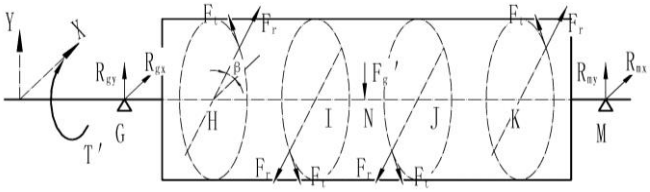

Figure 8. Diagram of Force Analysis of Output Shaft

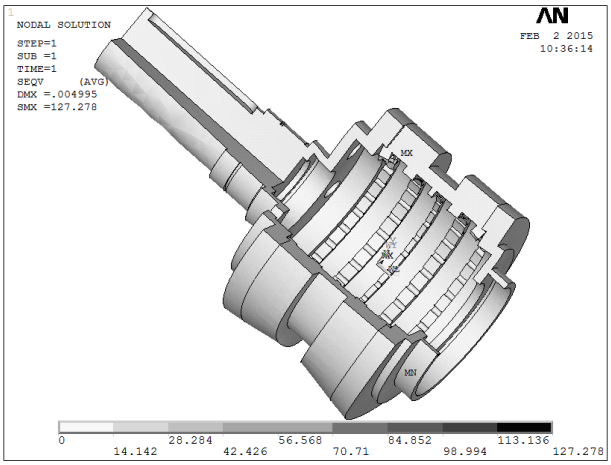

Figure 9. Finite Element Analysis of Output Shaft

Copyright ⓒ 2015 SERSC

Where, F_g' is weight of output shaft. The force condition of output shaft is as similar as input shaft, four sets of contact forces are balanced also.

Hence, $R_{gx} = R_{mx} = 0$, $R_{gy} = F_g' \cdot L_{GN} / L_{GM}$, $R_{my} = F_g' \cdot L_{NM} / L_{GM}$.

The output shaft, supported flange and pin-wheel are import into ANSYS as a finite element model, which is shown in Figure 9. Conditions of constraint and force include: First, we define the constraint of point M in the following way: restrict the freedoms of radial and axial directions. And then we restrict the freedom of radial direction of point G. Second, circumferential force Ft and radial force Fr are set on the nodes of element model that are corresponding points H, I, J and K in Figure 8. Those forces are not concentrated on a point, but a series of discrete forces act on seven pins of pin-wheel (Specific forces are shown in Figure 2.). Finally, we set the output torque on the nodes of model and output the stress distribution of output shaft as shown in Figure 9.

The calculating conditions and analysis results of output component are listed in Table 4. The calculating stress of output component can be ignored, because the moment is small compared with its dimensions. Result of FEA is 127.3 *MPa*, the maximum stress is distributed on the holes of pins that is shown in Figure 9.

Table 4. Calculating Conditions and Analysis Results of Output Component

Circumferential force F_t (*N*)	5,361
Radial force F_r (*N*)	515
Output torque T ($N \cdot mm$)	1,243,752
Bending torque of output shaft M_{Imax}($N \cdot mm$)	184,000
Shear stress of outputshaft (*MPa*)	18.2
Maximum stress of FEA (*MPa*)	127.3

4. Efficiency Analysis

4.1. Generic Calculating Method of Planetary Trains Efficiency

The efficiency is one of major performances for this drive. The main influencing factors include: meshing efficiency η_c, bearing efficiency η_z and lubricating efficiency η_Y. Hence, the total efficiency can be expressed by $\eta = \eta_c \eta_z \eta_Y$ [25].

In the planetary transmission, the input power of driver can be expressed by N_a^c, where N_a^c >0, the output power of followers can be expressed by N_b^c, where N_b^c <0, where superscript C is ground. The generic calculating formulas is

$$\eta_{ab}^c = -\frac{N_b^c}{N_a^c} = -\frac{M_b}{M_a} \cdot \frac{n_b^c}{n_b^c} \quad (4)$$

Where M is the rotation torque and n is the rotation speed of corresponding components.

The power transfer from input shaft to output shaft experience three pairs of bearings, let us assume that the efficiency of a pair of bearing is $\eta_{bearing}$=0.99 on the base of statistical data, we obtain the $\eta_z = \eta_{bearing}^3$=0.97. If lubricant of reducer adopt grease that

 Copyright ⓒ 2015 SERSC

the friction of oil would not be considered, where the η_Y =1. Hence, meshing efficiency will be the major performance about the total efficiency.

4.2. Meshing Efficiency η_c

The drive is made up by three basic components of planetary gear trains. 1st component in Figure 1.b is the input shaft act as the ground in converted gear trains, 4th component fixed-pin is fixed on ground in original gear trains that will act as ground. 2nd component pin-wheel and output shaft are the same in converted trains and original trains, which act as movable component. So we can obtain the formulas of meshing efficiency.

1. As shown in Figure 1.b, 1st component is the drive component and 2nd component is output component when 4th component act as ground. Thus,

$$\eta_{12}^4 = -\frac{M_2}{M_1}\cdot\frac{n_2^4}{n_1^4} = -\frac{M_2}{M_1}i_{21}^4 = -\frac{M_2}{M_1}\cdot\frac{1}{z_p} \quad (5)$$

2. If we analyze the converted trains of output pin-wheel cycloid drive, in which the 1st component act as ground. We should analyze the transmission relationship i_{14}^2. If i_{14}^2>0, the 2nd component in Eq.5 will unchanged about the relationship of driver or follower, otherwise it will be inversed. The corresponding equation can expressed by $i_{14}^2 = \frac{n_1 - n_2}{n_4 - n_2}$, and the 4th component is ground, thus n_4 =0, $i_{14}^2 = -\frac{n_1}{n_2} + 1 = -z_p + 1$, the result will not more than zero certainly. So the relationship of driver or follower will be inversed, where

$$\eta_{24}^1 = -\frac{M_4}{M_2}\cdot\frac{n_4^1}{n_2^1} = -\frac{M_4}{M_2}i_{42}^1 = -\frac{M_2}{M_1}\cdot\frac{z_p}{z_c} \quad (6)$$

On the base of principles of three basic components, where M_1+M_2+M_3=0. Hence, the corresponding equation of meshing efficiency derived from Eq.5 and Eq.6 is

$$\eta_{12} = -(\eta_{24}^1\cdot\frac{z_c}{z_p} - 1)^{-1} / z_p \quad (7)$$

Where, η_{24}^1 is friction efficiency of cycloidal gear and pins, the average range is from 0.997 to 0.998.

4.3. Calculation Example

Calculating the transmission efficiency of prototype, let η_{24}^1=0.997. Substitute η_{24}^1 into eq.7, hence the meshing efficiency is $\eta_{12} = -(0.997\cdot\frac{28}{29} - 1)^{-1} / 29 \approx 0.9225$. Let η_z =0.97, thus the total efficiency is about η =89.5 %. So it will be a kind of high efficiency drive.

5. Conclusions

In summary all the above sections, the output pin-wheel cycloid planetary drive is a kind of transmission device that have the high loading capacity and well dynamic performances. It has the advantages includes: small volume, light weight, wide range of transmission ratio and high efficiency, etc. the disadvantages of several planetary drives are improved by structural innovation and optimal design. Based on the analysis of working principle and design method for this drive, the systematic

Copyright ⓒ 2015 SERSC

design principle and analysis methods are established. So the preparation of manufacture for the prototype is done.

Hence, we obtain the following conclusions

1. The rotating torque and power can be doubled compared with traditional cycloid reducer. Hence, the power per unit mass would be increased and the cost of products would be decreased.
2. The structure of output shaft is changed from cantilever to simply supported beam, as a result the force condition is improved and the rigidity and strength of shaft is increased.
3. The transmission efficiency is approaching to 90%, so the economy and using prospects are wide in the future.

Acknowledgements

We are grateful for the support provided by the National Science Foundation of China (No. 51375064) and financial support of Department of Education of Liaoning Province (No. L2013192)

References

[1] W. He, L. Li, W. Wei and Y. Liu, "Study on Dynamic Response Optimization and Experiment of the Double Crank Ring-Plate-Type Pin-Cycloidal Gear Planetary Drive", Proceedings of 2010 International Conference on Advances in Materials and Manufacturing Processes, **(2010)** November 6-8; Shenzhen, China.

[2] J. Bao and W. He, "Dynamics simulations of virtual prototypes of double crank ring-plate-type pincycloidal gear planetary drive with three gears", Proceedings of 2010 International Conference on Computer Application and System Modeling, **(2010)** October 22-24; Taiyuan, China.

[3] Y. Zhang, W. He and X. Yang, "Dynamical formulation and analysis of double crank ring-plate-type pin-cycloidal gear planetary drive", 2010 International Conference on Frontiers of Manufacturing and Design Science, **(2010)** December 11-12; Chongqing, China.

[4] Y.-L. Jin, W.-D. He, L.-X. Li and J.-Y. Ding, "Tooth profile optimization and kinematic simulation of double crank ring-plate-type pin-cycloidal gear planetary drive", Journal of Northeastern University, vol. 5, no. 26, **(2005).**

[5] L. Lei, X. Shi and T. Guan, "Finite element analysis for cycloid gear and pin teeth of FA cycloid drive based on ANSYS", Proceedings of 2nd International Conference on Advanced Design and Manufacturing Engineering, **(2012)** August 16-18; Taiyuan, China.

[6] Y. Li and C. Zhu, "Analysis of the Multi-Tooth Meshing Effect of Three-Ring Gear Reducer", Proceedings of 2nd International Conference on Mechanical Engineering and Green Manufacturing, **(2012)** March 16-18; Chongqing, China.

[7] Y. Li, "Three-Dimensional Design and Motion Simulation of the Three-Ring Gear Reducer", Proceedings of 2nd International Conference on Advances in Materials and Manufacturing Processes, **(2012)** December 16-18; Guilin, China.

[8] J. Bao, W. He, Q. Lu and L. Li, "Research of Output-Pin-Wheel Cycloid Drive Reducer", Proceedings of 2010 WASE International Conference on Information Engineering, **(2010)** August 14-15; Beidaihe, China.

[9] J. H. Lee, N. Gu, M. J. Ostwald and J. Jupp, "Understanding cognitive activities in parametric design", Proceedings of 15th International Conference on Computer-Aided Architectural Design Futures, **(2013)** July 3-5; Shanghai, China.

[10] R. Anderl and R. Mendgen, "Parametric design and its impact on solid modeling applications", Proceedings of Proceedings of the 3rd Symposium on Solid Modeling and Applications, **(1995)** May 17-19; New York, United States.

[11] M.-A. Schnabel, "Parametric designing in architecture: A parametric design studio", Proceedings of 12th Computer-Aided Architectural Design Futures Conference, **(2007)** July 11-13; Sydney, Australia.

[12] J. M. Jauregui-Becker and W. O. Schotborgh, "A decomposition algorithm for parametric design", Proceedings of 18th International Conference on Engineering Design, **(2011)** August 15-18; Copenhagen, Denmark.

[13] S. Brell-Cokcan and B. Johannes, "A new parametric design tool for robot milling", Proceedings of 30th Annual Conference of the Association for Computer Aided Design in Architecture, **(2010)** October 21-24; New York, United states.

 Copyright ⓒ 2015 SERSC

[14] P. Von-Lockette, D. Acciani, J. Courtney, C. Diao, W. Riddell, K. Dahm and R. Harvey, "Bottle rockets and parametric design in a converging-diverging design strategy", Proceedings of 113th Annual ASEE Conference and Exposition, **(2006)** June 18-21; Chicago, United states.
[15] E. Oberg, F. D. Jones, H. L. Horton and H. H. Ryffel, C. J. Mccauley, "Machinery's handbook", Industrial Press, New York **(2008).**
[16] S. Budynas-Nisbett, "Mechanical Engineering", McGraw-Hill Companies, America **(2008).**
[17] W. He, X. Li, and L. Li, "Journal of Dalian Railway Institute", Study of a double crank four ring-plate cycloid drive driven by double motors, vol. 1, no. 26, **(2005).**
[18] B. Yang and Y. Liu, "Acta Armamentarii", Vibration and noise reduction of a double crank four ring-plate-type cycloid speed reducer, vol. 10, no. 32, **(2011).**
[19] X. Zhang and D. Shujing, "The input axis' mode analysis of the four ring-plate-type cycloid gear planetary drive", Proceedings of 2012 International Conference on Advances in Mechanics Engineering, **(2010)** August 3-5; Hong Kong, China.
[20] J. Sun, "Pro/Engineer Virtual Design and Assembly", China Railway Press, Beijing **(2004).**
[21] A. Olshevsky Alexander, A. Olshevsky Alexey and K. V. Shevchenko, "FEM simulation of inelastic contact of rough bodies", Proceedings of 2nd International Conference on Heterogeneous Material Mechanics, **(2008)** June 3-8; Huangshan, China.
[22] M. Bohuslav, H. Pavel and S. Ctibor, "FEM analyses of connections for several structures of a hydraulic radial forging machine", Proceedings of 21st International DAAAM Symposium "Intelligent Manufacturing and Automation", **(2010)** October 20-23; Zadar, Croatia.
[23] H. Zhu, L. Zhu and J. Chen, "Study of damage mechanism on aluminum alloy under two kinds of stress states and FEM simulation", Proceedings of Asian Pacific Conference for Fracture and Strength, (**2007)** November 22-25; Sanya, China.
[24] G. Mamtimin and K. Masanori, "Key Engineering Materials. Shape optimization of metal welded bellows seal based on the turing reaction-diffusion model coupled with FEM", **(2008),** pp. 385-387.
[25] X. Li, W. He, Li. Schmidt and L. Li, "Chinese Journal of Mechanical Engineering (English Edition)", Efficiency analysis of double crank ring-plate-type pin-cycloidal gear planetary drive, vol. 3, no. 16, **(2003).**

Authors

Junhua Bao, he received the Ph.D. degree in Mechanical Manufacturing and Automation from Dalian Jiaotong University, Dalian, China, in 2012. He is currently a Assistant Professor of Department of Mechanical Engineering, Dalian Jiaotong University. His current interests include computer aided design, mechanical design and simulation.

Weidong He, he received the Ph.D. degree in Mechanical Design and Theory from Harbin Institute of Technology, Harbin, China, in 1999. He is currently a Professor of Department of Mechanical Engineering, Dalian Jiaotong University. His current interests include computer aided design, mechanical design and simulation.

Copyright ⓒ 2015 SERSC

Copyright ⓒ 2015 SERSC